# Supporting Information

## Designing Bithiazole-Based Conjugated Polymers as Alternatives to Benzothiadiazole for Photocatalytic Hydrogen Evolution

Taekmin Kim,[a†] WonJo Jeong,[b†] Sanghyeok An,[a] Junho Kim,[d] Gayoung Ham,[c] Seungok Pyo,[b] Hyojung Cha,[c*] In Hwan Jung,[b*] and Dae Sung Chung[a*]

[a] Department of Chemical Engineering, Pohang University of Science and Technology (POSTECH), Pohang 37673, Republic of Korea. E-mail: dchung@postech.ac.kr

[b] Department of Organic and Nano Engineering, and Human-Tech Convergence Program, Hanyang University, Seoul 04763, Republic of Korea. E-mail: inhjung@hanyang.ac.kr

[c] School of Energy Engineering, Kyungpook National University, Daegu 41566, Republic of Korea. E-mail: hcha@knu.ac.kr

[d] Department of Energy Engineering, Hanyang University, Seoul 04763, Republic of Korea

* Corresponding authors

## Experimental

### 1. Material Synthesis

### 1.1. Synthesis of 4-octyl-2-(4'-octyl-[2,2'-bithiophen]-5-yl)thiazole (Compound 1)

2-Bromo-4-octylthiazole (1.01 g, 3.66 mmol), 2,5-bis(trimethylstannyl)thiophene (0.750 g, 1.83 mmol), and tetrakis(triphenylphosphine)palladium(0) (0.11 g, 0.09 mmol) were dissolved in toluene (40.0 mL). After purging with $N_2$, the mixture was refluxed for 48 hours. The reaction mixture was cooled to room temperature and extracted with dichloromethane (DCM) and water. The organic layer was dried over anhydrous $MgSO_4$, and the solvent was removed under reduced pressure. The resulting residue was purified by column chromatography on silica gel (DCM:hexane = 1:2, v/v). The product was recrystallized using DCM and MeOH to yield a yellow solid (0.68 g, 78.0%).

$^1$H-NMR (400 MHz, $CDCl_3$), δ (ppm): 7.442 (s, 2H), 6.825 (s, 2H), 2.782 (t, 4H), 1.735 (m, 4H), 1.380–1.278 (m, 20H), 0.883 (m, 6H)

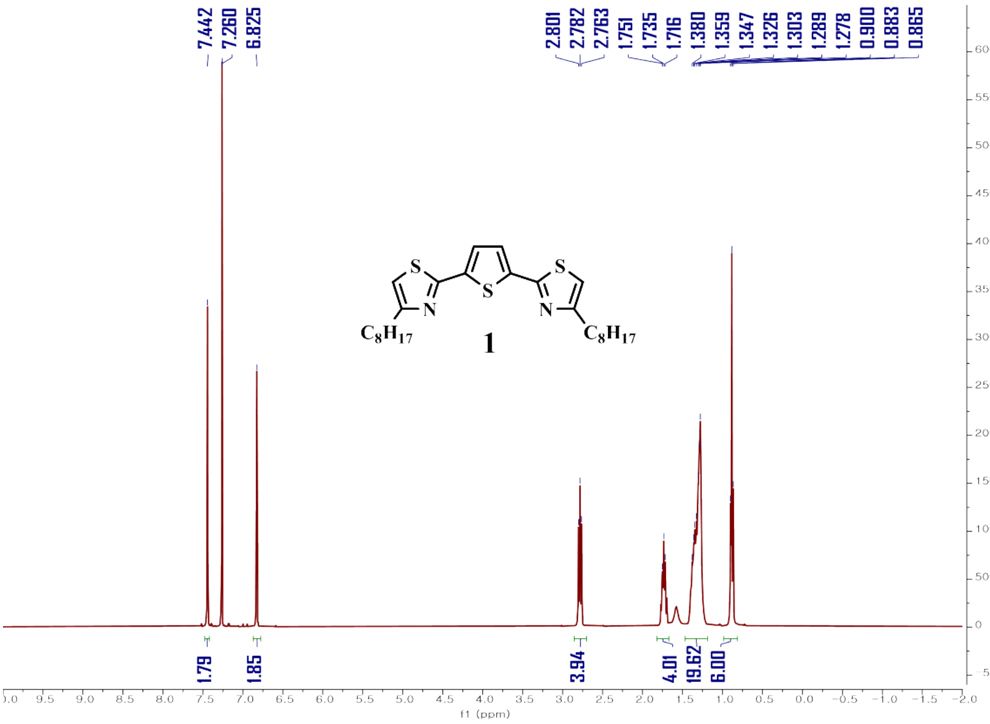

**Figure S1**. $^1$H NMR spectra of compound 1.

### 1.2. Synthesis of 2,5-bis(5-bromo-4-octylthiazol-2-yl)thiophene (Compound 2)

Compound 1 (1.00 g, 2.1 mmol) and N-bromosuccinimide (NBS) (0.94 g, 5.3 mmol) were dissolved in dimethylformamide (DMF) (60 mL). The mixture was stirred at room temperature overnight and then poured into water. The organic layer was extracted with DCM and water, dried over anhydrous $MgSO_4$, and concentrated. The residue was purified by column chromatography on silica gel (DCM:hexane = 1:2, v/v). The product was recrystallized using DCM and MeOH to yield a yellow solid (1.06 g, 80.0%).

$^1$H-NMR (400 MHz, $CDCl_3$), δ (ppm): 7.324 (s, 2H), 2.726 (t, 4H), 1.711 (p, 4H), 1.336–1.252 (m, 20H), 0.881 (t, 6H)

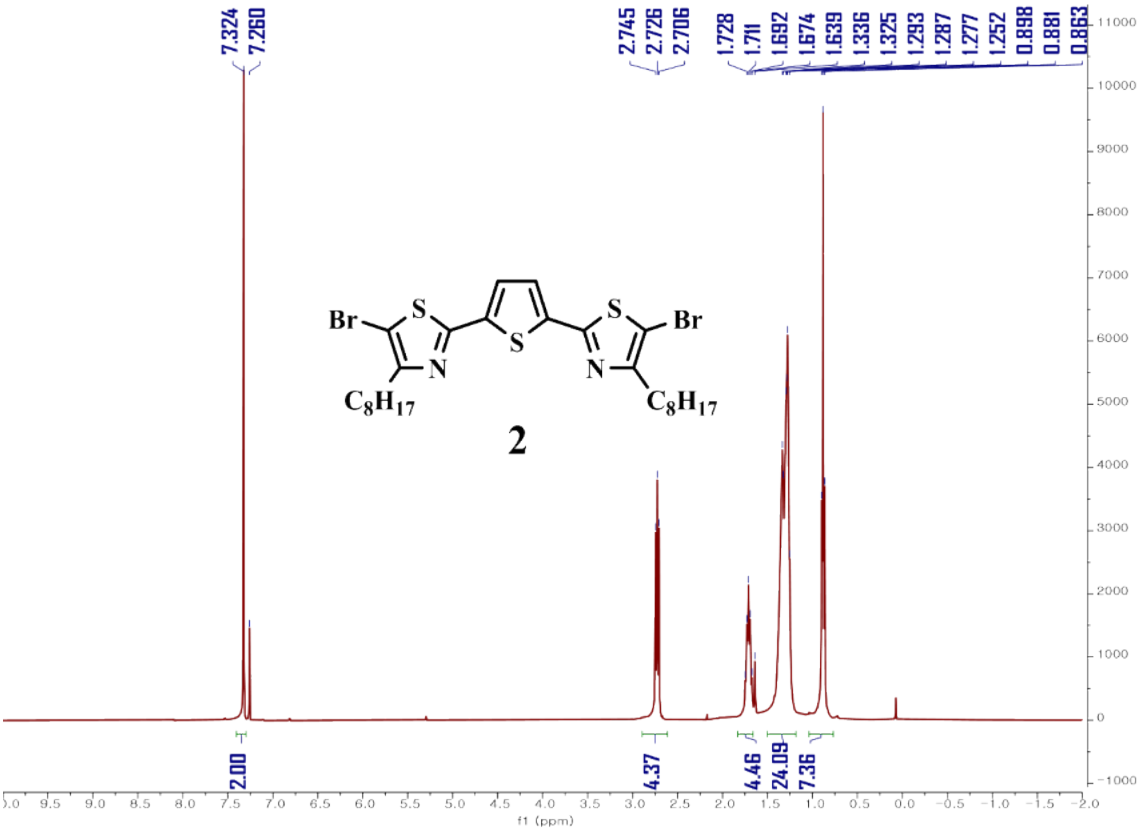

**Figure S2**. $^1$H NMR spectra of compound 2.

### 1.3. Synthesis of 4,4'-dioctyl-2,2'-bithiazole (Compound 3)

1-Bromooctan-2-one (1.00 g, 4.82 mmol) and dithioxamide (0.27 g, 2.29 mmol) were dissolved in ethanol (25.0 mL). After $N_2$ purging, the mixture was refluxed for 6 hours and then cooled to room temperature. The mixture was poured into cold water and extracted with DCM. The organic layer was dried over anhydrous $MgSO_4$. The residue was purified by column chromatography on silica gel using DCM. The product was obtained as a yellow solid (0.80 g, 89.0%).

$^1$H-NMR (400 MHz, $CDCl_3$), δ (ppm): 6.945 (s, 2H), 2.805 (t, 4H), 1.733 (p, 4H), 1.375–1.273 (m, 20H), 0.877 (t, 6H).

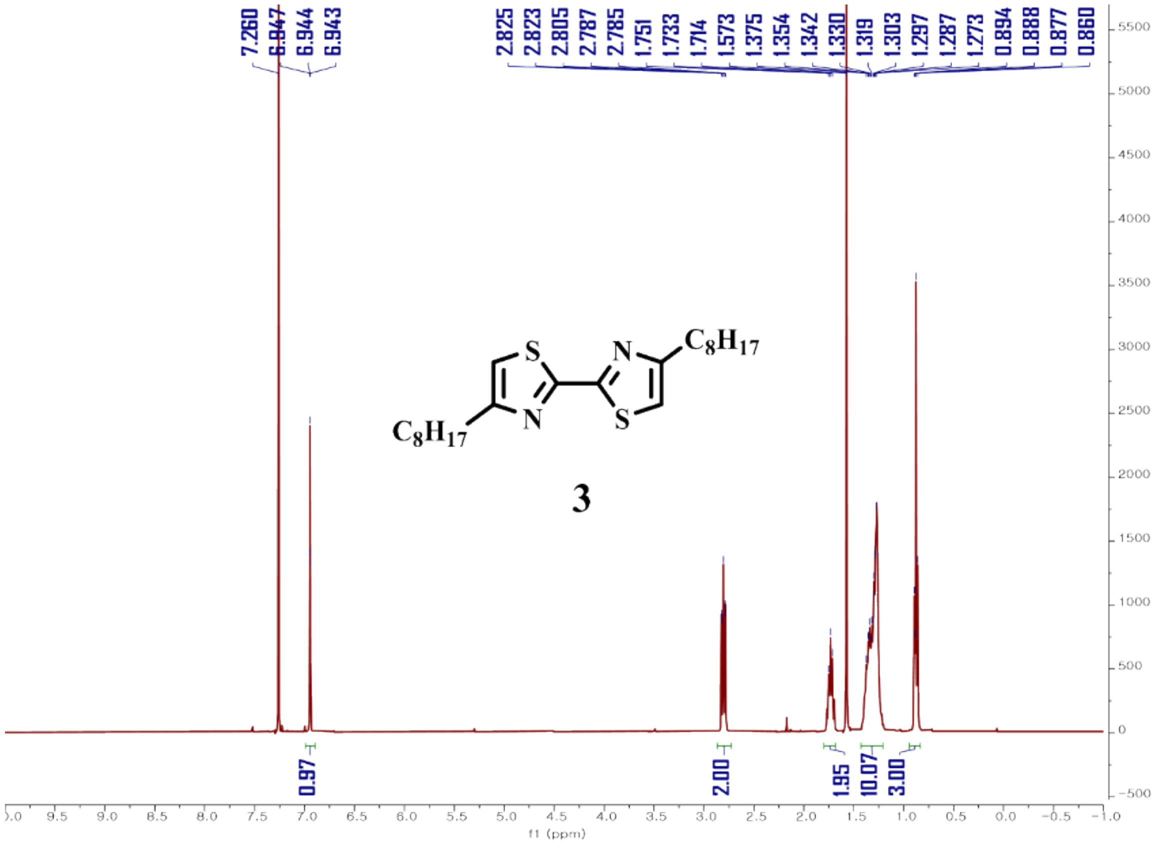

**Figure S3**. $^1$H NMR spectra of compound 3.

### 1.4. Synthesis of 5,5'-dibromo-4,4'-dioctyl-2,2'-bithiazole (Compound 4)

Compound 3 (0.50 g, 1.27 mmol) was dissolved in glacial acetic acid (15.0 mL) and DMF (15.0 mL). After purging with $N_2$ in the dark, NBS (0.45 g, 2.55 mmol) was added in portions. The mixture was stirred in the dark for 6 hours. The precipitate was filtered, washed with methanol, and purified by column chromatography (DCM:hexane = 1:3, v/v) to yield a yellow solid (0.65 g, 93.0%).

$^1$H-NMR (400 MHz, $CDCl_3$), δ (ppm): 2.740 (t, 4H), 1.697 (p, 4H), 1.327–1.249 (m, 20H), 0.878 (t, 6H)

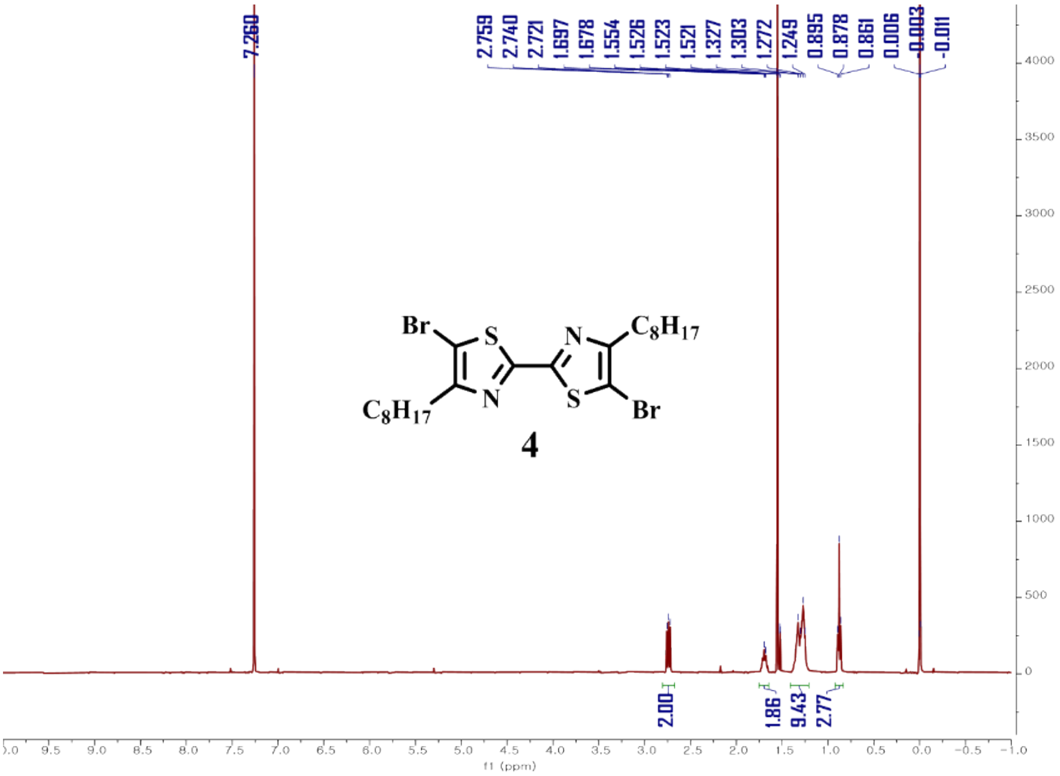

**Figure S4**. $^1$H NMR spectra of compound 4.

### 1.5. Synthesis of PFOTzT

Compound 2 (0.189 g, 0.30 mmol), fluorene (0.192 g, 0.30 mmol), and tetrakis(triphenylphosphine)palladium(0) (10 mg, 0.05 eq) were dissolved in degassed toluene (5.0 mL) with Aliquat® 336 (2 drops). Upon reaching 90 °C, degassed aqueous 2.0 M $K_3PO_4$ (0.435 mL, 4.3 eq) was added. After 4 days, bromobenzene (0.3 mmol) was added for end-capping. The mixture was poured into methanol, and the precipitate was dissolved in chloroform and filtered through Celite to remove the metal catalyst. Polymer fibers were washed by Soxhlet extraction with methanol, acetone, hexanes, and chloroform. The final product was obtained by reprecipitation from methanol (0.259 g, 91.0%).

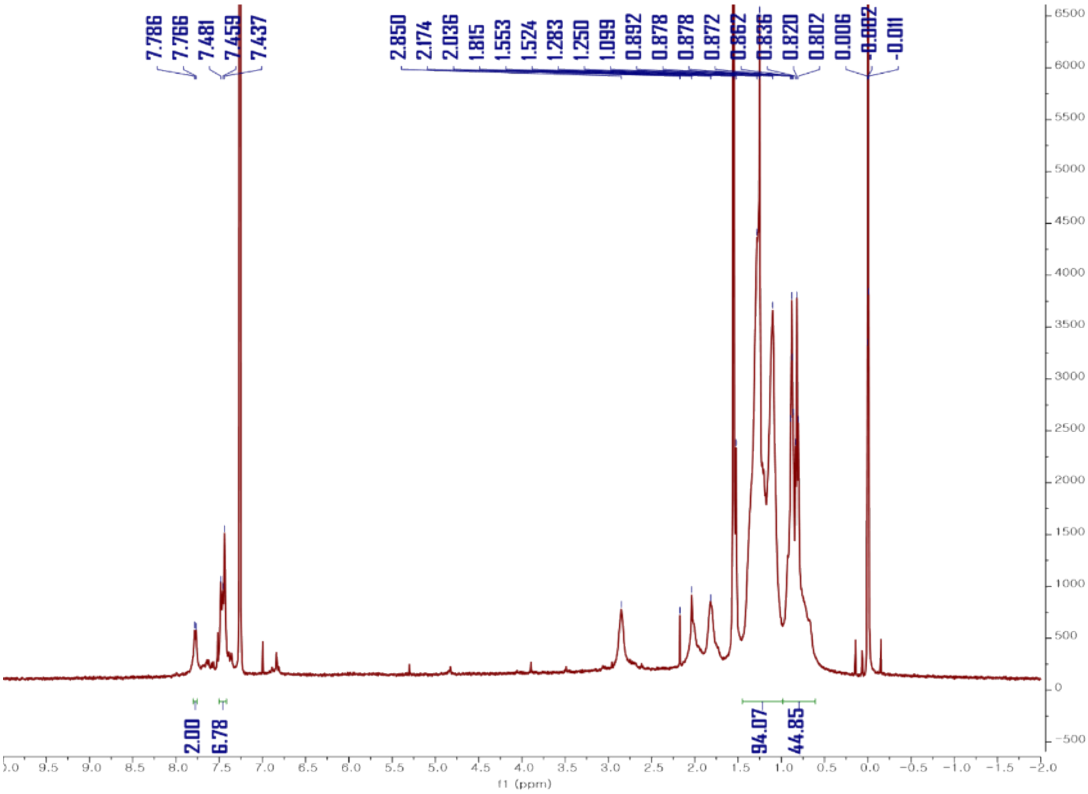

**Figure S5.** $^1$H NMR spectra of PFOTzT.

## Molecular Weight Averages

| Peak # | RT (min) | Mp (g/mol) | Mn (g/mol) | Mw (g/mol) | Mz (g/mol) | Mz+1 (g/mol) | PD |
|---|---|---|---|---|---|---|---|
| 1 | 5.640 | 101387 | 59066 | 212082 | 584732 | 1065114 | 3.590594 |

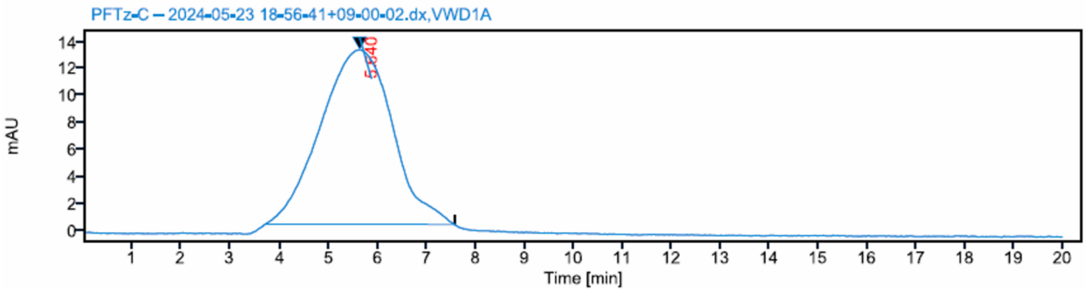

**Figure S6**. Gel permeation chromatogram of PFOTzT.

### 1.6. Synthesis of PFOTz

Compound 4 (0.165 g, 0.30 mmol), fluorene (0.192 g, 0.30 mmol), and tetrakis(triphenylphosphine)palladium(0) (10 mg, 0.009 mmol) were dissolved in degassed toluene (5.0 mL) with Aliquat® 336 (2 drops). At 90 °C, degassed aqueous 2.0 M $K_3PO_4$ (0.435 mL) was added. After 4 days, bromobenzene (0.3 mmol) was added for end-capping. The mixture was poured into methanol, and the precipitate was dissolved in chloroform and filtered through Celite. The polymer was purified by Soxhlet extraction (methanol, acetone, hexanes, and chloroform) and reprecipitated from methanol (0.234 g, 87.0%).

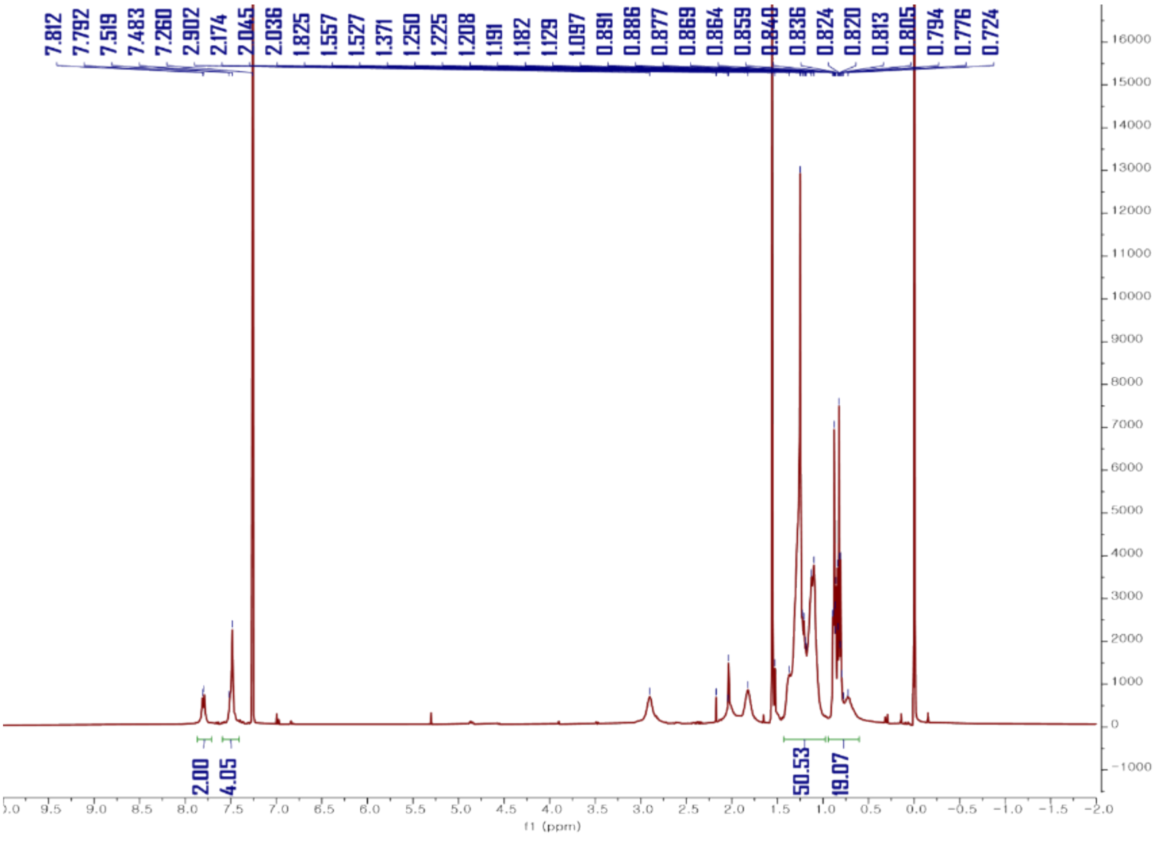

**Figure S7.** $^1$H NMR spectra of PFOTz.

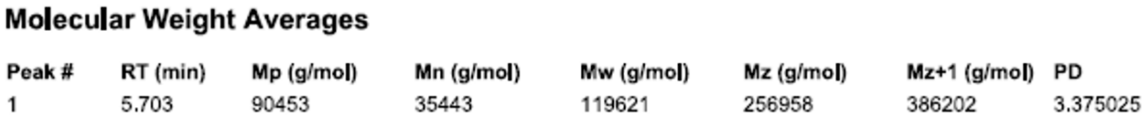

**Molecular Weight Averages**

| Peak # | RT (min) | Mp (g/mol) | Mn (g/mol) | Mw (g/mol) | Mz (g/mol) | Mz+1 (g/mol) | PD |
|---|---|---|---|---|---|---|---|
| 1 | 5.703 | 90453 | 35443 | 119621 | 256958 | 386202 | 3.375025 |

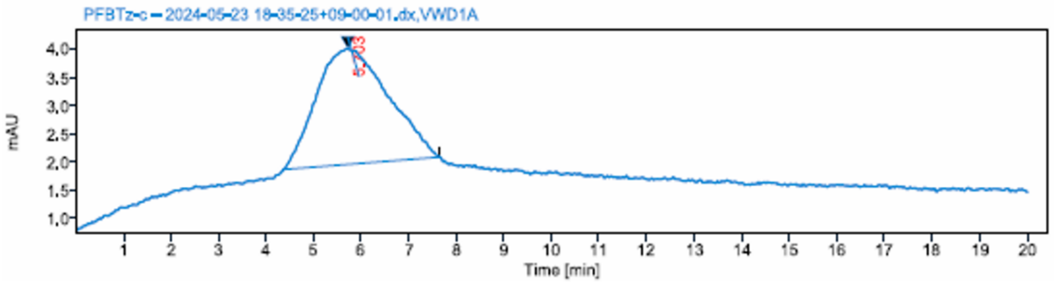

**Figure S8**. Gel permeation chromatogram of PFOTz.

## 2. Nanoparticle Synthesis via Mini-emulsion, Nanoprecipitation

### 2.1. Mini-emulsion

Nanoparticles were prepared by dispersing polymer solutions into an aqueous surfactant phase via high-energy ultrasonication. Briefly, polymers were dissolved in chloroform at a concentration of 1 mg mL$^{-1}$ (1 mL) and gently heated to 40 °C for 1 hour to facilitate complete dissolution. This organic phase was introduced into a 2 mL aqueous solution of SDS or TEBS (prepared by dissolving 50 mg of surfactant in 10 mL of deionized water). The resulting mixture was diluted with additional deionized water to yield a total volume of 8 mL and emulsified using a probe-type ultrasonicator (VibraCell VCX-750, 750 W) operated at 20% amplitude for approximately 10 minutes. The mini-emulsion was then heated on a hot plate at 75 °C to remove chloroform under ambient pressure. Any oversized aggregates present in the dispersion were removed by filtration through a 0.4 µm PTFE syringe filter.

### 2.2 Nanoprecipitation

For the nanoprecipitation route, polymers (1 mg mL$^{-1}$ in THF, 800 µL) were pre-mixed with PS-PEG-COOH (4 mg mL$^{-1}$ in THF, 800 µL) to form a homogeneous precursor solution. This solution was rapidly injected into 12 mL of deionized water under vigorous stirring. The resulting mixture was subjected to ultrasonication for 10 minutes to enhance dispersion. THF was then removed by heating the mixture at 85 °C for 90 minutes while continuously purging with nitrogen at a slow flow rate. The final colloidal suspension was filtered using a 0.4 µm PTFE membrane to eliminate any large particles or aggregates.

## 3. UV-Visible Spectroscopy

A Thermo Scientific Evolution 220 UV–vis spectrophotometer was used to obtain the UV–visible absorption spectra.

## 4. Cyclic voltammetry (CV)

Cyclic voltammetry measurements were performed at a scan rate of 20 mV/s using a WonATech potentiostat/galvanostat/impedance analyzer ZIVE SP1(1A), with a three-electrode cell and a 0.1 N Bu4NBF4 solution in acetonitrile as the electrolyte, and the working electrode was coated with the polymer films by dipping them into their solutions in chloroform. All measurements were calibrated against an internal standard of ferrocene (Fc), whose ionization potential is −4.8 eV for the Fc/Fc+ redox system.

## 5. Dynamic Light Scattering (DLS)

The size distribution of each nanoparticle batch was measured with a Malvern Zetasizer Nano S (Malvern Instruments Nordic AB). Average data were obtained from at least five runs of measurements.

## 6. Hydrogen Evolution Rate (HER)

Photocatalytic hydrogen evolution experiments were carried out in a sealed 50 mL quartz reaction vessel. The photocatalyst suspension was prepared by mixing nanoparticle dispersion (800 μL), deionized water (400 μL), and ascorbic acid solution (0.5 M pH 4 buffer NaOH, 800 μL) as the sacrificial electron donor. After thorough mixing, the reaction vial was tightly sealed and purged with argon gas for 30 minutes to remove dissolved oxygen. The suspension was then irradiated using a 300 W Xe arc lamp (Newport 6258, ozone-free) equipped with a 420 nm long-pass optical filter under continuous magnetic stirring. The evolved hydrogen gas was analyzed using a Nexis GC-2030 gas chromatograph with a thermal conductivity detector (TCD), calibrated using standard hydrogen gas. Dissolved hydrogen and pressure-related volume corrections were not included in the final calculations.

## 7. Steady-state Photoluminescence (SS-PL) and Time-resolved Photoluminescence (TR-PL)

The SS-PL and TR-PL data were measured with an FS5 spectrofluorometer (Edinburgh Instrument, Livingston, UK). The TR-PL was obtained using the time-correlated single-photon-counting (TCSPC) method with an excitation wavelength of 520 nm and 540 nm.

## 8. ns- µs Transient Absorption Spectroscopy (TAS)

The ns-µs TA data were collected using a pump – probe TA spectroscopy, which consisted of a TA spectrometer and a regenerative amplified Nd:YAG laser (EL-YAG) with a pulse width of 6-8 ns. The pulse is capable of generating both visible pulses (532 nm) and UV pulses (355 nm) through a third harmonic generator. The TA spectra data were collected over a time range from 6 ns to 500 ns. The probe beam is derived from a 150 W Xenon lamp, which is reflected off the nanoparticle sample and then passed through a monochromator before reaching a PMT-980 photodiode detector. To simultaneously capture data on two different time scales, the comprehensive L900 spectrometer software (V9.4.3) package is utilized, and the nanosecond-microsecond signal is sampled using an oscilloscope (Tektronix MDO30232, Beaverton, OR, USA). Excitation fluences are measured using a pyroelectric energy senor.

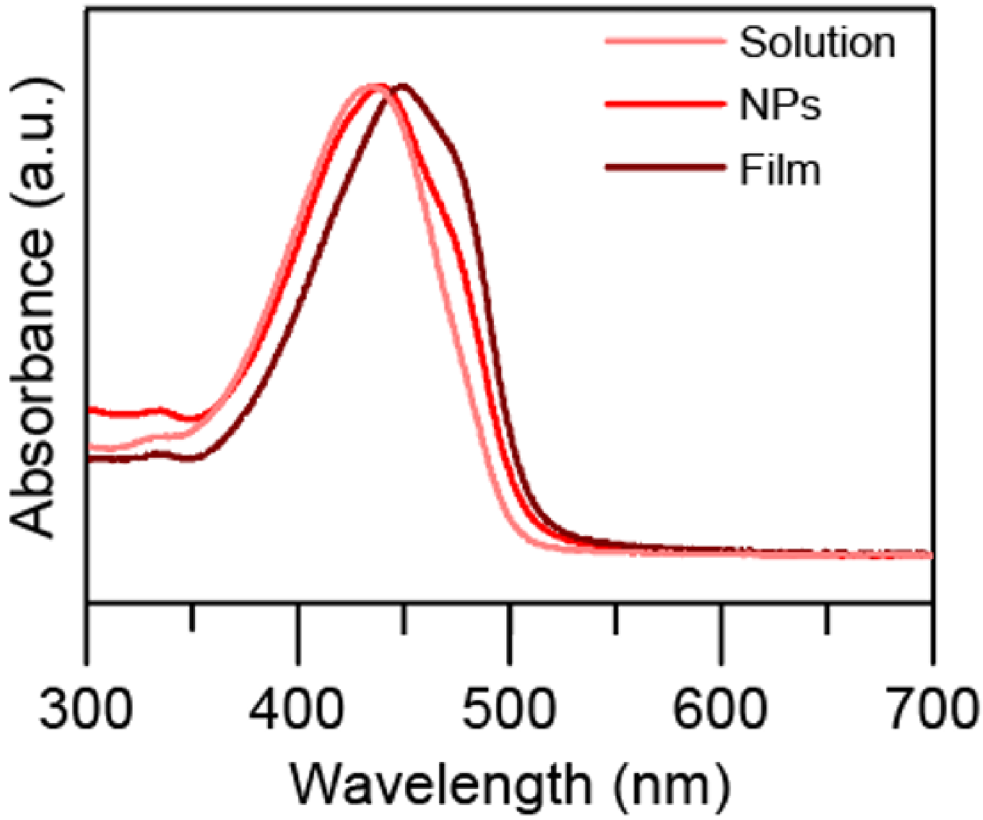

**Figure S9**. UV–Vis absorption spectrum of PFOTzT Solution, NPs, Film

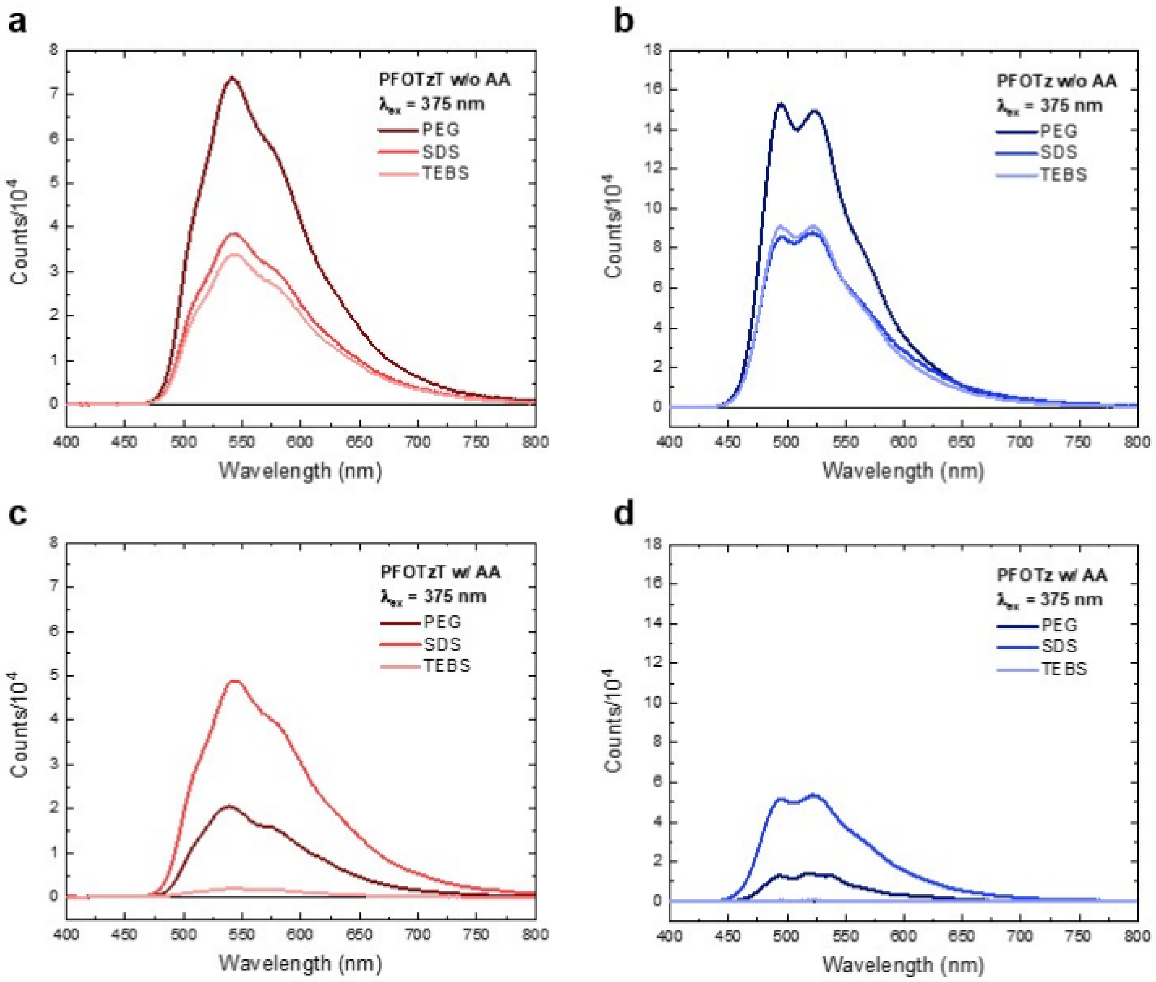

**Figure S10**. Steady-state PL spectra of PFOTzT and PFOTz nanoparticles measured before (a, b) and after (c, d) the addition of ascorbic acid (AA). All samples were excited at 450 nm.

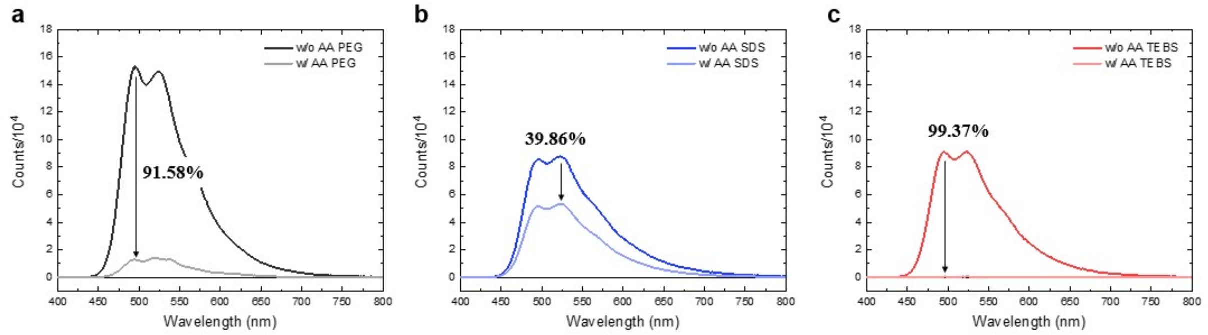

**Figure S11**. Exciton quenching yield evaluated by steady-state PL spectra of PFOTz nanoparticles stabilized with (a) PEG-COOH, (b) SDS, and (c) TEBS, under identical conditions.

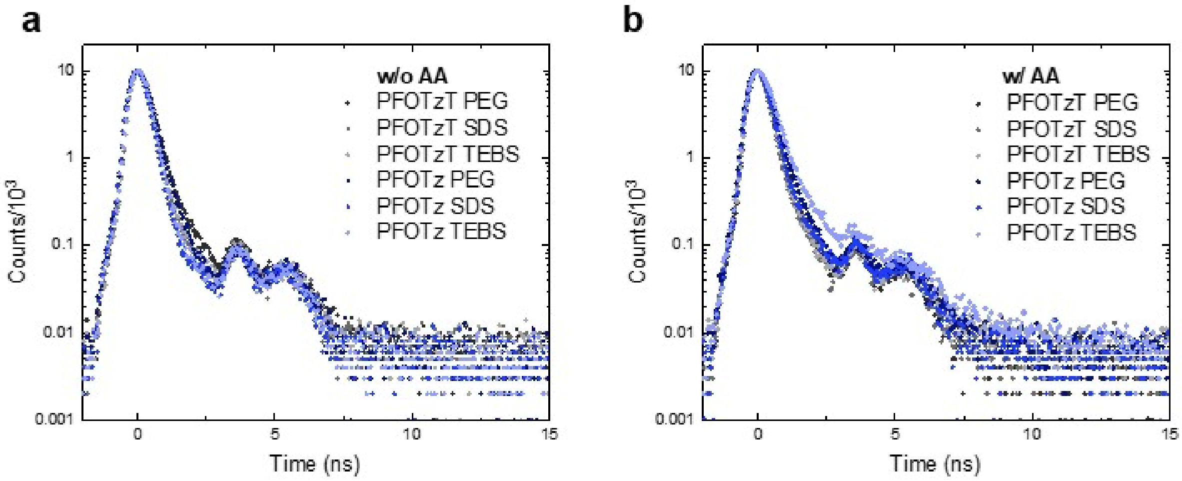

**Figure S12**. Time-resolved photoluminescence (TRPL) decay profiles of PFOTzT and PFOTz nanoparticles excited at PL maximum individually.

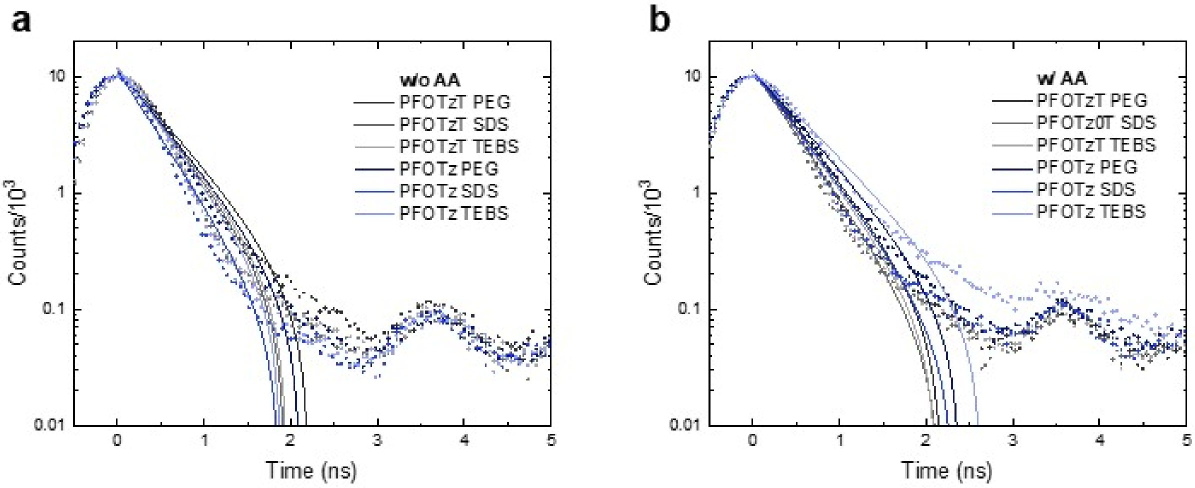

**Figure S13**. Expanded TRPL decay curves (0–5 ns) of PFOTzT and PFOTz nanoparticles with fitted trend lines

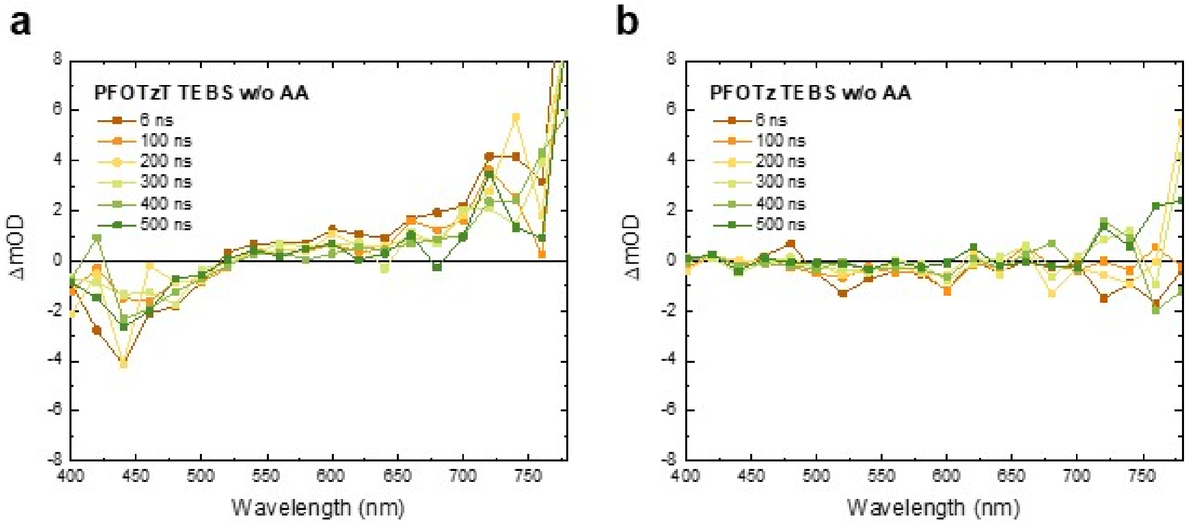

**Figure S14**. Comparison of transient absorption spectra between PFOTzT and PFOTz nanoparticles at various delay times post-355 nm excitation.

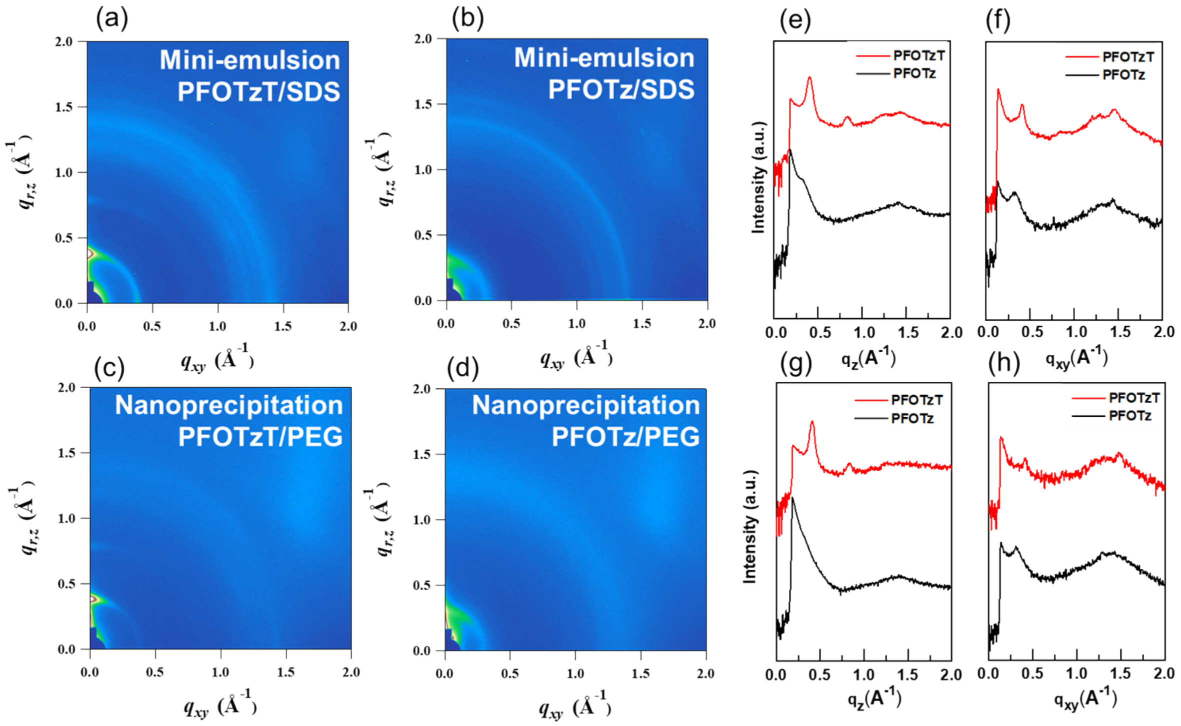

**Figure S15**. 2D-GIXD images for a) PFOTzT/SDS, b) PFOTz/SDS, c) PFOTzT/PEG, d) PFOTz/PEG. The line-cut data from e,f) SDS and g,h) PEG treatment.

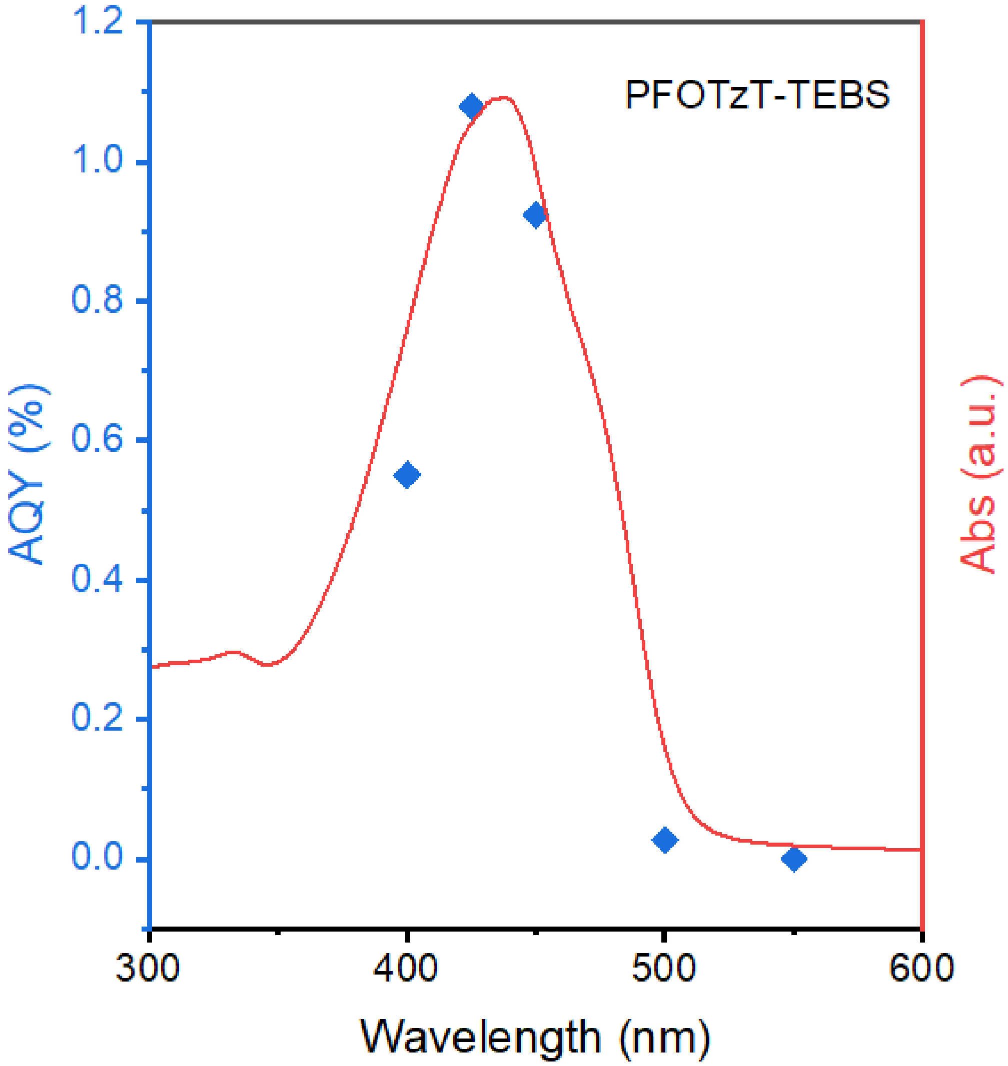

**Figure S16**. The wavelength-dependence of apparent quantum yield (AQY) for PFOTzT-TEBS

**Table S1.** Summary of hydrogen evolution rates (HER) and key kinetic parameters derived form transient absorption (TA) decay profiles.

| Polymer/Surfactant | Condition | Decay Half-life ($\tau_{1/2}$, ns) | Quenching Efficiency ((w/o AA) / (w/ AA)) | HER ($mol \cdot g^{-1} \cdot h^{-1}$) |
|---|---|---|---|---|
| PFOTzT/TEBS | w/o AA | ~800 | - | 246.8 |
| | w/ AA | 10 | >99% | - |
| PFOTzT/PEG | w/o AA | ~900 | - | 181.9 |
| | w/ AA | ~ | <5% | - |
| PFOTzT/SDS | w/o AA | ~1000 | - | 102.4 |
| | w/ AA | N/A | N/A | - |

**Table S2.** Summary of HER performance

| Material | Component | Co-catalyst | HER (mmol·g$^{-1}$·h$^{-1}$) | Reference |
|---|---|---|---|---|
| F8BT (BT-based polymer) | Single | Palladium | 0.140 | S1 |
| P10 | Single | Palladium (7000ppm) | 5.3 | |
| P3HT | Single | Palladium + Platinum | - | |
| P28 | Single | Palladium | 0.204 | S2 |
| PM6:Y6 | Multi | Platinum | 43.9 | *S3* |
| PFODTBT:ITIC (BT-based) | Multi | Platinum | 80.0 | *S4* |
| P4EOBDT-TTE:PCBM | Multi | Platinum | 164.3 | *S5* |
| PFBT (BT-based polymer) | Single | None | 60.5 | *S6* |
| PFOTzT | Single | None | 0.247 | This work |

References

S1. M. Sachs, H. Cha, J. Kosco, C. M. Aitchison, L. Francàs, S. Corby, C.-L. Chiang, A. A. Wilson, R. Godin, A. Fahey-Williams, A. I. Cooper, R. S. Sprick, I. McCulloch and J. R. Durrant, *J. Am. Chem. Soc.*, 2020, **142**, 14574–14587.

S2. R. S. Sprick, L. Wilbraham, Y. Bai, P. Guiglion, A. Monti, R. Clowes, A. I. Cooper and M. A. Zwijnenburg, *Chem. Mater.*, 2018, **30**, 5733–5742.

S3. J. Kosco, S. Gonzalez-Carrero, C. T. Howells, T. Fei, Y. Dong, R. Sougrat, G. T. Harrison, Y. Firdaus, R. Sheelamanthula, B. Purushothaman, F. Moruzzi, W. Xu, L. Zhao, A. Basu, S. De Wolf, T. D. Anthopoulos, J. R. Durrant and I. McCulloch, *Nat. Energy*, 2022, **7**, 340–351.

S4. A. Liu, S. Wang, H. Song, Y. Liu, L. Gedda, K. Edwards, L. Hammarström and H. Tian, *Phys. Chem. Chem. Phys.*, 2023, **25**, 2935–2945.

S5. L. Tian, S. Guo, L. Feng, J. Wang, A. Wang and C.-x. Cui, *J. Mater. Chem. A*, 2024, **12**, 32164–32171.

S6. P. B. Pati, G. Damas, L. Tian, D. L. A. Fernandes, L. Zhang, I. B. Pehlivan, T. Edvinsson, C. M. Araujo and H. Tian, *Energy Environ. Sci.*, 2017, **10**, 1372–1376